# Species-specific design of artificial promoters by transfer-learning based generative deep-learning model

Yan Xia[1], Xiaowen Du[1], Bin Liu[2], Shuyuan Guo[1*], Yi-Xin Huo[1,3*]

[1] *Key Laboratory of Molecular Medicine and Biotherapy, School of Life Science, Beijing Institute of Technology, 100081 Beijing, China;*

[2] *School of Computer Science and Technology, Beijing Institute of Technology, Beijing, China*;

[3] *Tangshan Research Institute, Beijing Institute of Technology, 063611 Hebei, China;*

[*]Corresponding authors. E-mail addresses: guosy@bit.edu.cn (S. Guo) huoyixin@bit.edu.cn (Y.-X. Huo).

**Abstract**

Native prokaryotic promoters share common sequence patterns, but are species dependent. For understudied species with limited data, it is challenging to predict the strength of existing promoters and generate novel promoters. Here, we developed PromoGen, a collection of nucleotide language models to generate species-specific functional promoters, across dozens of species in a data and parameter efficient way. Twenty-seven species-specific models in this collection were finetuned from the pretrained model which was trained on multi-species promoters. When systematically compared with native promoters, the *Escherichia coli*- and *Bacillus subtilis*-specific artificial PromoGen-generated promoters (PGPs) were demonstrated to hold all distribution patterns of native promoters. A regression model was developed to score

generated either by PromoGen or by another competitive neural network, and the overall score of PGPs is higher. Encouraged by *in silico* analysis, we further experimentally characterized twenty-two *B. subtilis* PGPs, results showed that four of tested PGPs reached the strong promoter level while all were active. Furthermore, we developed a user-friendly website to generate species-specific promoters for 27 different species by PromoGen. This work presented an efficient deep-learning strategy for *de novo* species-specific promoter generation even with limited datasets, providing valuable promoter toolboxes especially for the metabolic engineering of understudied microorganisms.

## Introduction

Regulating gene expression is essential to metabolic and biosynthetic engineering, as it enables the optimization of the production of desired metabolites, biofuels, pharmaceuticals, and other valuable compounds (1-4). Promoters are core regulatory elements that initiate the gene transcription, regulate gene expression, and affect metabolic flux distribution in metabolic pathways (5,6). By obtaining well-understood and user-friendly promoters, scientists could redesign cells to create gene circuits and synthetic biological systems tailoring to specific requirements (7). Although have been utilized to regulate gene expressions, native promoters lack continuous regulatory strength and wide regulatory scope (8). Therefore, many efforts have been made to develop artificial or hybrid promoters for regulating gene expressions (9-11).

The field of promoter engineering utilized random and semi-rational mutagenesis

43 techniques to develop promoter libraries (12,13) that containing promoters with varied
44 expression levels. For example, error-prone PCR based random mutagenesis was
45 applied to the PL-λ promoter in *Escherichia coli*, leading to a substantial 196-fold
46 variation in promoter activity identified through high-throughput screening (14). This
47 approach has also been successfully applied to other organisms, including *Lactococcus*
48 *lactis*, *Pichia pastoris*, and *Saccharomyces cerevisiae* Tef1 to generate active promoters
49 (15-17). On the other hand, semi-rational design has been used to engineer *Bacillus*
50 *subtilis* synthetic promoter libraries to obtain promoters with transcriptional activities
51 varying up to 100-fold by fixing the -10 and -35 regions and altering the flanking
52 regions of promoters $P_{veg}$, $P_{ser\mathrm{A}}$, and $P_{ymd\mathrm{A}}$ (16,18). Although engineered promoters
53 with enhanced performance have been reported, challenges remained in generating and
54 screening large-scale libraries for obtaining promoters with a broad and continuous
55 range of strengths (8).

56 Deep learning architectures have shown substantial promise for the manipulation
57 of both eukaryotic and prokaryotic promoter elements. These sophisticated models
58 excelled in generating a lot of functional promoters by assimilating and analyzing the
59 information of distribution patterns inherent in extensive native promoter sequences
60 (19,20). For example, synthetic promoters were *de novo* generated by Generative
61 Adversarial Networks (GANs) and 70.8% generated promoters showed activities in *E.*
62 *coli*, utilizing a 14,098 experimentally validated promoters as a training dataset (21). In
63 a recent advancement, this model has been refined to not only produce entire promoter

sequences but also to generate flanking regions while maintaining the integrity of the core regions in *E. coli* and mammalian cells (22). Meanwhile, a Variational Autoencoder (VAE) was trained to generate synthetic promoters of varying efficiency in cyanobacteria using 3,712 promoter sequences that identified through differential RNA sequencing (dRNA-seq) (23). These models demonstrated that robust performance could be achieved in the presence of extensive and high-quality experimental data. As the scope of metabolic engineering broadens to encompass an array of non-model prokaryotic organisms, the dearth of comprehensive and high-quality datasets emerges as a formidable challenge.

Recently, the field of text generation has witnessed significant advancements through the application of transfer learning, which combined Generative Pre-trained Transformers (GPT) with instruction datasets for the purpose of fine-tuning (24-26). This approach was exemplified by the success of ChatGPT (**Figure 1A**). In the pre-training phase, the model learns general and distribution patterns from a multitude of unlabeled datasets. Thereafter, a fine-tuning process, steered by data related to specific tasks, equips the model to efficiently adapt to a variety of application contexts (26). This methodology was particularly efficient in scenarios where data was limited, as transfer learning effectively augmented the precision of model and adaptability in such data-scarce situations (25). Biological sequences including proteins and nucleotides are regarded similar to natural languages as both of them use a set of symbols to represent information (27,28). Some nucleotide language models, e.g. DNABert, Nucleotide

85 Transformers, GENA-LM, HyenaDNA (27-29), were designed to understand the
86 genetic information. Transferrable understandings of sequences from genome could be
87 learned by nucleotide language models, which were trained on existing genome
88 sequences. However, most nucleotide language models are BERT-like models trained
89 to learn representations of nucleotide sequences rather than to generate new sequences
90 (30). One of the current challenges in developing generative model is to benchmark the
91 quality of the generated sequences. Typically, the evaluation of sequence quality relies
92 on scores of third-party *in silico* models and experimentally verification *in vivo* or *in*
93 *vitro*. *In silico* evaluations commonly have a much higher throughput than experiments
94 *in vivo* or *in vitro*, but experimental data are more reliable (31).

95 To address the challenge of insufficient promoter data of certain species, we
96 designed a pre-trained model based on Transformer, termed the PromoGen-pre. This
97 model was further refined with species-specific promoter data to yield 27 distinct
98 promoter-generating models for both model and non-model species. To validate the
99 effectiveness of our strategy, we evaluated the key characteristics of the generated
100 promoters including position weight matrix, 6-mer frequency correlation and -10 region
101 distribution in *E. coli* and *B. subtilis*. We developed a scoring model to evaluate the *E.*
102 *coli* promoters generated by our model and WGAN-GP, demonstrating the
103 competitiveness of our model. Most of the generated promoters exhibited confirmed
104 activities in *B. subtilis*. An online webserver was developed to enhance the accessibility
105 of the promoter-generative models where users could generate *de novo* promoters for

106 27 different species based on the PromoGen model. The related models and analysis
107 methods were listed in Supplementary Table S1. Via aforementioned transfer learning
108 approach for generating new promoters from scratch, we expanded the available
109 promoters for a specific species and offered potential candidates for use in metabolic
110 engineering even when the available data was limited.

111 **Results**

112 **PromoGen-pre is a generative pre-trained model for promoter sequences**

113 Unsupervised language models have become the foundation of current advancement in
114 the natural language processing (NLP) field (32). Language model could be built and
115 trained based on the large number of unlabeled data, and be improved via transfer-
116 learning for performing downstream tasks with task-specific dataset. Transfer-learning
117 dependent strategy, which has been successfully exploited to generate functional
118 proteins across diverse families recently, has yet been reported to generate new
119 functional DNA elements. To investigate the potential of transfer learning on generating
120 DNA regulatory elements, we developed a decoder-only Transformer-based model,
121 termed PromoGen-pre, to specifically capture the characteristics of prokaryotic
122 promoter sequences (**Figure 1B**). Unlike the conventional byte-pair encoding (BPE) or
123 k-mer tokenization strategy (33,34), the DNA sequences were tokenized at the character
124 level in PromoGen-pre to ensure that the original location of each base in the DNA
125 sequence was kept within the position of each token, allowing the DNA generation
126 more controllable (**Supplementary Figure S1A**). The tokenized input sequence was

127 embedded as numerical representation $X_{emb} \in \mathbb{R}^{L \times D}$, where $L$ is the sequence length
128 and $D$ is the dimension of the hidden vector of each token. PromoGen model further
129 updated the numerical representation though GPT2Blocks with multi-head self-
130 attention (**Figure 1B, Supplementary Figure S1B**) (25).

131 When predicting the next token, the long-distance relation across the sequence
132 would be taken account by PromoGen-pre via the self-attention mechanism.
133 PromoGen-pre was trained by autoregressive approach, where the probability of each
134 nucleotide in the sequence was conditioned solely on the upstream nucleotides. Cross-
135 entropy loss was utilized to evaluate and adjust the performance of PromoGen-pre
136 during the model training process. The 10 million tokens from more than 129k
137 sequences that containing experimentally verified promoters and Transcriptional Start
138 Sites (TSS) in the Prokaryotic Promoter Database (PPD), which is one of the most
139 comprehensive promoter sequence databases containing sequences from more than 27
140 species, were subjected to the pretraining of PromoGen **(Figure 1C, D)** to ensure the
141 high quality and reduced deviation (**Figure 2A, 2B**) (35).

142 After the above training, we observed that the promoters from the same species
143 were clustered close to each other when the sequence representations encoded by
144 PromoGen-pre model were projected to a two-dimensional plan, indicating that the
145 model has learned to distinguish the promoters by species in the absence of supervision
146 related to species information (**Figure 2C**). For example, the sequences from *Haloferax*
147 were notably well distinguished from other species by PromoGen, highlighting the

148 differences of regulatory elements between Archaea and Bacteria (**Figure 2C**) and
149 confirming that PromoGen-pre is able to encode meaningful promoter representations.
150 On the other hand, some projected points representing promoters from different species
151 were also gathered together in the Figure 2C, indicating that some promoters from
152 distinguished species are sharing common patterns which is in agreement with the well-
153 known observation that bacteria are able to recognize certain heterologous genetic
154 elements. This observation reinforced our rationale to tackle the low-data challenge by
155 transfer learning.

156 Since PromoGen-pre has been trained to obtain meaningful representations from
157 native promoters, we investigated whether the trained PromoGen-pre could generate
158 functional artificial promoters. The results showed that the projected points of artificial
159 promoters generated by PromoGen-pre (pink points in Figure 2C) was dispersedly
160 distributed within, and did not form obvious cluster outside of, the ones of native
161 promoters, indicating that the generated promoters were likely to be functional as the
162 native ones. So far, the generated promoters were not species specific although the pre-
163 training stage allowed PromoGen-pre to learn the comprehensive features of promoters
164 from different species, encompassing a broader spectrum and evolutionary information.

165 Although previous works developed a collection of benchmarks including
166 eighteen genomic related prediction tasks (27), we find it is still challenging to evaluate
167 whether nucleotide language models could understand prokaryotic promoters because
168 currently only mouse and human promoters were involved in the benchmarks. On the

169 other hand, only promoter sequences, but not genomic chunks, were provided to
170 PromoGen-pre for training, making PromoGen-pre being intrinsically capable of
171 distinguishing native promoters and random sampled genomic chunks, which was a
172 challenging task for other models. Therefore, a benchmark dataset based on
173 experimentally verified synthetic promoters was needed for PromoGen-pre.

174 We first evaluated the ability of PromoGen-pre to distinguish whether a generated
175 sequence is a promoter in a zero-shot manner (36). The log-likelihood of each sequence
176 was calculated by PromoGen-pre to a predicted score. As a comparison, we also
177 evaluated the performance of the nucleotide transformer family models (NTFM) which
178 have number of parameters range from 50 million (M) to 2.5 billion (B) NTFM enabled
179 precise prediction of molecular phenotypes based on learned patterns from DNA
180 sequences (27). We computed the area under the receiver operating characteristic
181 (auROC) curves to predict the binary label from scores (37). The results showed that
182 the PromoGen-pre, a small model with solely 7.4 M parameters, has log-likelihood
183 auROC of 0.60, equally well, (if not better than) as the same level of the 2.5 B model
184 (**Figure 2D**), better than the Nucleotide Transformer 50 M, 100 M, 250 M, and 500 M.
185 This result showed that a relatively small amount of project-related high-quality data
186 could fulfill the task, enabling PromoGen to reach the performance of large model
187 trained with large dataset.

188 **Finetune the pre-trained model based on datasets from 27 species**

189 PromoGen-pre has been trained on multiple prokaryotic promoter sequence datasets,

endowing it with the capability to generate promoters for various species. To adapt the model for species-specific applications, we conducted fine-tuning based on the datasets of 27 major species in the dataset, resulting in the development of 27 distinct promoter models, encompassing species such as *E. coli*, *B. subtilis*, *Sinorhizobium*, *Corynebacterium*, and so on. Such transfer learning methodology facilitated the development of a robust promoter generative model even with relatively small-size datasets.

Taking *E. coli* model as an example to evaluate the effectiveness of transfer learning, we then tried to score and compare the generation quality of PromoGen-eco and a GAN-based WGAN-GP model through independent predictive models which were designed to predict activities of promoters. To select the most reliable predictive model for predicting the activities of the generated promoters, we evaluated twelve machine learning based predictive models by calculating metrics including MAE, RMSE, Spearman correlation coefficient, and Pearson correlation coefficient (**Supplementary Figure S2**). the Bayesian Bridge model was selected as our final predictive model because it consistently demonstrated exceptional performance no matter which calculation methods were used for evaluation. The Bayesian Bridge model achieved a Spearman correlation coefficient of 0.69 or 0.58, and a Pearson correlation coefficient of 0.70 or 0.60 on training and test data, respectively, demonstrating the accuracy of this model (**Figure 3A, 3B**).

We generated 200 promoter sequences by PromoGen-eco and WGAN-GP,

211 individually, and used Bayesian Bridge prediction model to predict the promoter
212 activities of these 400 promoters (21). As depicted in figure 3C, the average score of
213 PromoGen-eco generated promoters was significantly higher compared to the ones
214 generated by WGAN-GP, indicating the strong capability of PromoGen-eco in *de novo*
215 promoter generation. In addition, another prediction model employed in previous study
216 (21), Deep Promoter CNN, was utilized to assess the performance of PromoGen-eco.
217 The results indicated that PromoGen-eco exhibited high competitiveness when
218 compared with WGAN-GP (**Supplementary Figure S3**). Furthermore, analysis
219 utilizing PWM revealed that the promoters generated by PromoGen-eco exhibited a
220 distribution identical to that observed in native promoters while the distribution of
221 promoters generated by WGAN-GP displayed slight variations from the native
222 distribution (**Supplementary Figure S4**). To evaluate the similarity between natively
223 occurring promoters and those synthesized by PromoGen-eco, we counted the hexamer
224 frequencies of the promoters. The resulting Pearson and Spearman correlation
225 coefficients were 0.954 and 0.965, respectively, indicating a high degree of similarity
226 in the 6-mer frequency between the generated and native promoters (**Figure 3D**). These
227 findings collectively suggested that PromoGen-eco has successfully captured the
228 characteristics and distribution patterns of *E. coli* promoters, showcasing its strong
229 capability in *de novo* promoter generation.

230 **Performance evaluation of PromoGen-bsu model**

231 To further validate the effectiveness of various species specific PromoGen models, we

232 performed promoter prediction and activity evaluation in *B. subtilis,* a species with
233 higher promoter selectivity and is an important Gram-positive bacterium used in protein
234 production and chemical manufacturing. We fine-tuned PromoGen-pre using 691
235 promoter sequences from *B. subtilis* to obtained PromoGen-bsu, which was then
236 utilized to generate *B. subtilis* specific promoters (**Supplementary Figure S5**). To
237 assess the quality of generated promoters, PromoGen-bsu generated promoters were
238 randomly sampled and compared with native ones and PromoGen-pre generated ones.
239 We utilized PWMs to depict the sequence motifs within the promoter regions derived
240 from native sources, as well as those synthesized by PromoGen-pre and PromoGen-bsu
241 (**Figure 4A**). Our investigation revealed a conserved motif within the -10 box,
242 extending from position -13 to -8 in the native promoters. The conservation of this motif
243 aligns with earlier studies conducted on a variety of bacterial species, including *B.*
244 *subtilis*, *E. coli*, and cyanobacteria. Notably, in the -10 region of the PromoGen-bsu-
245 generated promoters, we detected a sequence pattern mirroring that of the native
246 promoters, suggesting that PromoGen-bsu has successfully replicated the essential
247 features of this -10 motif. Additionally, the -35 region, located at the positions of -36 to
248 -31, exhibited partial conservation in both the natively occurring and PromoGen-bsu-
249 constructed promoter sequences. Contrasting with this, the sequence of PromoGen-pre
250 attributes exhibited substantial deviation from the native *B. subtilis* promoters,
251 exhibiting only a marginal preference for T, A bases within the -10 region and no
252 preference within -35 region.

253 We conducted a quantitative assessment of hexamer frequencies in both natively
254 occurring promoters and those generated by PromoGen-pre and PromoGen-Bsu. The
255 analysis revealed a moderate correlation between the hexamer frequencies of native
256 promoters and those generated by PromoGen-pre, as indicated by Pearson and
257 Spearman correlation coefficients of 0.508 and 0.199, respectively. Conversely, a
258 significantly higher correlation was observed in sequences produced by PromoGen-bsu,
259 with Pearson and Spearman coefficients of 0.900 and 0.733, respectively, illustrating a
260 closer alignment with the hexamer frequency patterns found in native promoters
261 (**Figure 4B**). We noted a substantial consistency in high-frequency 6-mers between the
262 native and PromoGen-bsu generated promoters, specifically including sequences like
263 TAAAAT and TATAAT that encompass the -10 box. We also investigated the distance
264 distribution of TAAAAT and TATAAT sequences relative to the transcription start site
265 (TSS) (**Figure 4C**). The analysis of the promoters synthesized by both PromoGen-pre
266 and PromoGen-bsu revealed a distinguishable accumulation of hexamers, particularly
267 in the -10 region. This region exhibited a significantly higher frequency of these
268 sequences compared to other areas, aligning with the distribution observed in native
269 promoters. The sequences generated by PromoGen-bsu having a higher portion of both
270 TATAAT and TAAAAT as the -10 region comparing to PromoGen-pre. These findings
271 underscored the capability of the PromoGen-bsu model to accurately replicate the
272 spatial distribution patterns of conserved motifs inherent to native promoters, thereby
273 affirming its efficacy in reflecting the native positional preferences of these sequences.

274 The t-SNE visualization in Figure 4D illustrated the arrangement of promoter
275 sequences, *i.e.* native, PromoGen-pre, and PromoGen-bsu, which were projected from
276 a high-dimensional landscape into a two-dimensional plane. In this representation, the
277 promoters generated by the pre-trained model, depicted as orange dots, were dispersed
278 throughout the space, predominantly occupying the right side, which suggestsed a
279 distinct pattern from the rest. In contrast, the native and PromoGen-pre -generated
280 promoters, represented by green and blue dots respectively, were intermingled and
281 uniformly situated on the left side. This indicated a shared distribution pattern among
282 them, showing the PromoGen-bsu has learned the related distribution in *B. subtilis*
283 promoters.

284 **The activity of generated promoters in *B. subtilis***

285 To assess the functionality of the synthesized promoters, we utilized PromoGen-bsu to
286 create 50 *de novo* designed promoters, each has 61 nucleotides in length (**Figure 5A**).
287 From this pool, 22 were arbitrarily chosen for experimental testing. As benchmarks, we
288 employed native promoters from *B. subtilis*, such as $P_{43}$, $P_{veg}$, and $P_{lepA}$, alongside three
289 random sequences to serve as controls, both positive and negative. We constructed 28
290 shuttle vectors expressing fluorescent proteins *sfGFP*, each harboring the replication
291 origins pBR322 and RepA for *E. coli* and *B. subtilis*, enabling *sfGFP* expression in both
292 hosts. The activities of the promoters were determined by the fluorescence intensity
293 emitted by *sfGFP*. Sampling was conducted during the logarithmic growth phase for
294 fluorescence measurement. A fluorescence reading higher or lower than that of the

295 randomly generated sequences indicated an active or inactive promoter, respectively.

296 As shown in Figure 5B, the results indicated that PromoGen-bsu could generate
297 active promoters although the strength of the promoters vary. Three random sequences
298 exhibited no activity. This result was expected because the range of promoter intensities
299 use in the training data vary also. Almost all of these promoters are active, with about
300 18% of them including A7, A9, A5, and A3 showed activities similar to the natively
301 strong promoters $P_{43}$ and $P_{veg}$. Notably, the A7 promoter stands out, exhibiting an
302 activity rate 91% higher than that of $P_{43}$. The strength of the other promoters varies,
303 allowing for different levels of gene expression to be achieved. The bacterial strains
304 expressed the *sfGFP* gene were subjected to observation under a fluorescence
305 microscope. Notably, these organisms demonstrated notable fluorescence when
306 compared to counterparts utilizing random sequences as promoters (**Supplementary**
307 **Figure S6**). Furthermore, our investigation encompassed the analysis of t-SNE
308 distribution patterns, compared experimentally tested 22 promoters with 691 natively
309 promoters in *B. subtilis*. This analysis showed that the generated promoters were quite
310 dispersed and were significantly distant from strong promoters, indicating a
311 considerable difference (**Figure 5C**). Examination of the five most potent promoters
312 uncovered a shared sequence, TTG, within the -35 region, and adjacent sequences were
313 identified spanning positions 17-18 bp between the -35 and -10 regions (**Figure 5D**).
314 Additionally, the activities of these promoters were tested in *E. coli.* The experimental
315 results demonstrated that all promoters were active in *E. coli*, with 64% showing

316 enhanced activity compared to *B. subtilis* (**Supplemental Figure S7**). This finding
317 further validates that our model generates sequences that are not random but
318 functionally significant in biological contexts. Moreover, these results support the
319 concept of the universality of prokaryotic promoters, as discussed in studies from 2018.
320 Our research also indicates that promoters in *B. subtilis* exhibit greater selectivity
321 compared to those in other species.

322 To assess the similarity of the generated promoters to native promoters, a
323 comprehensive BLAST analysis was performed, comparing the experimentally
324 validated promoters against the entire genome of *B. subtilis*. The results showed that
325 the generated sequences do not have similarity. This finding implies that the sequences
326 were predominantly *de novo* designed by the models, rather than being a result of data
327 leaks. This suggested that PromoGen-bsu has effectively captured the distribution
328 patterns of active *B. subtilis* promoters, exploring a sequence space of $4^{61}$ and
329 showcasing the ability to generate new active species-specific promoters.

330 **Development of a user-friendly web sever**

331 To facilitate the rapid generation of promoter sequences, we have developed an online
332 web server (https://promogen1.cloudmol.org/) providing fine-tuned models for 27
333 prokaryotic organisms. As shown in **Fig. 5E**, the promoter sequences could be
334 generated after choosing the specific organism. The number and length of the generated
335 promoters could be flexibly customized according to the needs. The generated results
336 were presented in a sequence that ranked them according to decreasing values of the

337 log-likelihood. The repetition penalty, Top P, and temperature were commonly utilized
338 hyperparameters for controlling the diversity and quality of text generation. By
339 increasing the repetition penalty, we could prevent the generative model from
340 producing multiple repeated tokens. This strategy not only mitigates the occurrence of
341 hallucinations in the generative model but also reduces the complexity involved in
342 constructing plasmids. By adjusting the temperature and Top P settings, the diversity of
343 the generated sequences could be regulated, thereby mitigating the risk of converging
344 on local minima. This online platform offers a user-friendly interface for creating
345 customized promoters for diverse species, serving specific needs and thereby
346 facilitating the efficiency of subsequent experimental and research activities.

347 **Discussion**

348 Regulatory elements play a crucial role in metabolic engineering (38). By selecting
349 appropriate promoters, we could precisely control the gene expression of specific
350 metabolic pathways, enhancing or inhibiting the fluxes of particular metabolic routes
351 to increase the production of target chemicals. Identifying and verifying appropriate
352 regulatory elements in understudied microbes is frequently a challenging and time-
353 consuming task (18). Deep learning offers a promising approach for generating
354 promoters from scratch or predicting the activity of existing promoters. However, the
355 limited data available for understudied microbes poses a significant barrier to the
356 effective utilization of deep learning models. Here, we proposed a fast and convenient
357 solution based on generative self-supervised nucleotide language model, capable of

358 generating promoters with different strengths. We employed a transfer learning strategy,
359 which pre-trained the model using promoter sequences mainly from 27 species to learn
360 the general patterns and paradigms of the promoters. Subsequently, fine-tuning was
361 performed using species-specific promoter data, resulting in promoter models
362 applicable to 27 different species. Our PromoGen was pretrained on multi-species data,
363 making its adaptation to other species easier than WGAN-GP, which was only trained
364 to generate *E. coli* promoters. Even for *E. coli* promoters, our PromoGen worked as
365 accurate as, if not better, than the existing WGAN-GP model. Furthermore, under core
366 region analysis and experimental validation, PromoGen-bsu model exhibited
367 exceptional performance, with all of the generated promoters showing activities.
368 Consistent results from model evaluation, key region analysis, and experimental
369 validation indicated that PromoGen successfully learned promoter distribution patterns
370 and could be used for generating entirely new promoters. For user convenience, an
371 online webserver was developed containing data for 27 species, allowing users to
372 quickly generate promoter sequences for their desired species.

373 The quality of the dataset plays a crucial role in the performance of deep learning
374 models. Transfer learning offers an excellent solution for small-scale datasets. An
375 increasing number of microorganisms are being used for various applications, but
376 research on regulatory elements lags behind in non-model microorganisms. By utilizing
377 the pre-trained model PromoGen-pre, we are able to reduce the data requirements for
378 deep learning models, making it possible to *de novo* generate promoters for species

379 with limited data. Although there are some differences in promoters among different
380 species, the characteristics of the core region of prokaryotic promoters have been well-
381 learned by the pretrained model PromoGen-pre. The activity of generated promoters
382 could be enhanced by fixing key positions. Although the training data is limited
383 comparing with other models, the information about promoter sequences is highly
384 enriched. We observed DNA sequences differently from natural language in these
385 aspects because there is no evidence that there is a pre-organized grammar across all
386 species beside the Watson-Crick pairs. We also demonstrated that the zero-shot
387 prediction accuracy of PromoGen-pre on promoter activities were comparable or higher
388 than the ones of other nucleotide transformer models which are 6 to 330 times bigger
389 than PromoGen-pre. We anticipated that this information enrich strategy would be
390 helpful to projects with limited resources.

391 Although previous reports and our work demonstrated that it is effective to design
392 promoters using generative models, it is challenging to assess the quality of generated
393 promoters. The current methods for assessing generated sequences primarily
394 encompass wet lab verification and computational experiment evaluation. Wet lab
395 verification is the most precise approach, though large-scale experimental validations
396 are time-consuming and labor-intensive. The evaluation methods for computational
397 experiments include using comparative sample distributions and benchmark testing.
398 Deep learning is capable of learning shallow features of data, which facilitates easy
399 overfitting to match the sample distribution. Therefore, biologists should focus on

establishing high-quality assessment datasets that are comprehensive, covering a wide array of scenarios and conditions, to guarantee the accuracy of evaluations.

Despite the fact that employing promoters of varying strengths is one of the most crucial methods for regulating gene expressions, the integration of diverse regulatory elements such as Ribosome Binding Sites (RBS), terminators, insulators, and others, offers expanded options for gene expression modulation (39-41). Furthermore, synthetic promoters, which establish a predetermined expression intensity, present challenges in dynamically regulating gene expression during growth. Promoters that are inducible or dependent on sigma factors could dictate the timing and intensity of gene activation. In the future, the design and development of pertinent models carry substantial promise for applications within the realm of synthetic biology.

In summary, we implemented a transfer learning strategy to address the challenges posed by a limited dataset. By the combination of pre-training and finetune, 27 species-generated models were developed for *de novo* design of promoter sequences, which were evaluated by prediction model and experiments validation as promoters with exceptional performance. Furthermore, we have developed a user-friendly web server that enables rapid generation of promoters. Our work provided a novel strategy and a universal pre-trained model PromoGen-pre, showcasing the potential of deep learning methods to explore the sequence space of regulation elements, especially in situations with limited data availability.

## METHODS

**Details of nucleotide language models**

The vocabulary of PromoGen contains 7 tokens, including four bases A, T, C, G, and special tokens including [PAD], [MASK], and [UNK]. By applying one-hot encoding, the input sequences are transformed into numerical vectors that can be processed by neural networks. The one-hot vectors are transformed into hidden state vectors of 320 dimensions:

$$x_{emb} = E(x_i) \tag{1}$$

To distinguish the positions of each token, a learnable positional embedding is added:

$$PE(pos, 2i) = sin\left(pos/10000^{2i/d_{model}}\right) \tag{2}$$

$$PE(pos, 2i+1) = cos\left(pos/10000^{2i/d_{model}}\right) \tag{3}$$

where the pos is the position of the context, i is the index of the dimension in the encoding vector, and the $d_{model}$ represents the dimensionality of the outputs in all layers of the model. This position embedding is followed the original design of the GPT2 model (24).

The longest sequence allowed is 128. The hidden vectors are updated by 6 layers of GPT2 Block (25). In a GPT2 block, the hidden vectors are updated with multi-head self-attention, and a feed forward layer, with residual connections:

$$Multihead\ Attention(\mathbf{Q}, \mathbf{K}, \mathbf{V}) = softmax\left(\frac{(QK^T)}{\sqrt{d_k}}\right)\mathbf{V} \tag{4}$$

**Q** is query matrix, **K** is key matrix, **V** is value matrix, and $d_K$ is dimension of the key vectors. $\mathbf{W_1}$ and $\mathbf{W_2}$ is Weight matrices of the linear transformations. $b_1$ and $b_2$ is bias terms of the linear transformations. The number of head in multi-head self-attention is set to 4.

$$FFN(x) = f(x\boldsymbol{W_1} + b_1)\boldsymbol{W_2} + b_2 \tag{5}$$

The feed forward layer (FFN) is consisted of two linear layers, to expend the dimension by a factor of 2 and activated using the Gaussian Error Linear Unit (GELU) function.

$$Output = LayerNorm\big(x + Sublayer(x)\big) \tag{6}$$

Residual connections and layer normalizations are applied in GPT2 block. The last hidden vectors are transformed to logits of tokens by the language modeling head, which is a linear layer has output dimension equal to the size of the vocabulary. The final output of the model is the probability of each base at the next position and generates promoter sequences by autoregression way from 5' to 3', one by one, which the next base has relied on all previously generated bases.

$$p(x) = \prod_{i=1}^{n} p(S_n | S_1, \dots, S_{n-1}) \tag{7}$$

**Training of nucleotide language models**

To train the PromoGen, we used 120k promoter sequences containing more than 27 species from the Prokaryotic Promoter Database (PPD). The PromoGen model is a model trained using the GPT-2 method (25). To efficiently train this model, the batch size was configured at 64, allowing for the simultaneous processing of 64 data samples. We predict the probability of each token based on previous context, comparing these predictions with actual data by computing cross-entropy loss to assess the prediction accuracy of model. To optimize the performance of model, the Adam optimizer was employed (42), renowned for its capability to dynamically adjust the learning rate, thereby bolstering the training efficiency and overall efficacy. We set several key parameters, including two decay rate parameters, β1 and β2, set to 0.9 and 0.999, respectively, and a constant called epsilon, set to $5e^{-4}$. During the fine-tuning phase, the

weights from the pre-trained model are utilized as initial values. We configure the batch size to be 32, and the learning rate for the Adam optimizer is set at $1e^{-5}$. Other parameters remain consistent with those established in the PromoGen configuration.

**Training and selection of predictive models**

We systematically evaluated 12 machine learning models to accurately predict the activity of promoters, including Extra Tree Regressor, Linear Regression, Gradient Boosting Regressor, Ada Boost Regressor, Ridge Lasso K-Neighbors Regressor, Random Forest Regressor, Bayesian Ridge, Support Vector Regression (SVR), eXtreme Gradient Boosting (XGB) Regressor, and Decision Tree Regressor (43-50). We extracted features from promoters using a nucleotide pre-trained model, employing the features from the [CLS] token as the representation for the entire sequence, which served as input to the machine learning models. To ensure a fair comparison of these methods, we conducted 5-fold cross-validation across the entire dataset ensuring independent predictions for all samples. At the same time, we calculated Mean Absolute Error (MAE), Root Mean Square Error (RMSE), Spearman correlation, and Pearson correlation coefficients (51,52).

To further enhance the accuracy of the predictive model, we conducted a hyperparameter search for the Bayesian Bridge model. These hyperparameters included maximum optimization iterations, alpha1, alpha2, lambda1, and lambda2, resulting in a total of $3^5$ combinations. Setting the maximum optimization iterations to 300 and alpha1, alpha2, lambda1 as $1e^{-7}$, and lambda2 as $1e^{-5}$ yielded the best performance in

488 cross-validation. These optimal hyperparameters were used to Bayesian Bridge model
489 for predicting promoter strength, ensuring our model achieves the highest level of
490 accuracy.

491 **The model evaluation by position weight matrix (PWM) and 6-mer frequency**
492 **analyses**

493 We performed multiple sequence alignment separately for both native and model-
494 generated promoter sequences. We calculated the weight for each position using a
495 formula:

496 $$W_{i,j} = log_2(\frac{f_{i,j}}{p_i}) \quad (8)$$

497 where $W_{i,j}$ represents the weight score of the $i$th base at position $j$. $f_{i,j}$ indicates the
498 relative frequency of the base at position $j$, and $p_i$ represents the background frequency
499 of that base. We utilized the obtained weight scores to create visualization using the
500 online website WebLogo.

501 In the analysis of 6-mer frequencies, we conducted a comprehensive scan of all 6-
502 mer sequences within both natural and synthetic promoters generated by PromoGen
503 and PromoGen-bsu, subsequently computing the frequency of each individual 6-mer.
504 During this process, particular attention was devoted to two pivotal 6-mer sequences,
505 TATAAT and TAAAAT, which frequently play crucial roles in the functionality of
506 promoters. To gain deeper insights into the representation of these key sequences across
507 various promoters, we specifically calculated their abundance distribution compared

508 with natural promoters.

509 **Plasmid construction**

510 This investigation employed a variety of plasmids, detailed in Supplementary
511 Table S2. All primer sequences were synthesized from Genewiz, located in Tianjin,
512 China (Supplementary Table S3). The shuttle plasmid, pXY43-sfGFP, was utilized as a
513 template, incorporating both pBR322 ori and repA ori for compatibility with *E. coli* and
514 *B. subtilis* respectively. A series of 22 generated promoter sequences were integrated
515 upstream of the superfolder green fluorescent protein (*sfGFP*) gene, replacing the
516 existing $P_{43}$ promoter via polymerase chain reaction (PCR) techniques. The amplified
517 PCR constructs were subsequently cultured on LB agar plates containing 50 μg $ml^{-1}$ of
518 kanamycin to facilitate clone selection. Three clones were selected to Sanger
519 sequencing for sequence verification in each plate. Furthermore, corresponding
520 plasmids containing the $P_{veg}$ and $P_{lepA}$ promoters from *B. subtilis* were also engineered,
521 alongside a set of plasmids with random sequences as promoters, to serve as negative
522 controls in the study.

523 **Fluorescence measurements**

524 The activity of these generated promoters was assessed based on the fluorescence
525 intensity emitted by *sfGFP*. The relevant promoter-plasmid were transformed into *B.*
526 *subtilis* strains, with single colonies subsequently cultivated in LB medium
527 supplemented with 20 μg $ml^{-1}$ kanamycin, maintained at 37°C and agitated at 220 r.p.m

528 (Supplementary Table S4). After an overnight growth, these cultures were then
529 transferred into fresh LB medium containing a 1% (v/v) inoculum, followed by an 8-
530 hour incubation at 37°C. The fluorescence intensity was quantitatively measured using
531 a microplate reader (BioTek) set at an excitation wavelength of 488 nm and an emission
532 wavelength of 507 nm. Concurrently, the cell optical density (OD) was detected at 600
533 nm. All these experimental procedures were replicated thrice to ensure reliability.

534 **Data availability:** All necessary data to assess the conclusions in the paper are
535 presented within the paper itself and/or the Supplementary Materials.

536 **Author contributions:** Y.-X.H., S.Y.G., and Y.X. conceptualized the project. Y.X.
537 designed, built, and implemented deep models in this study. Y.X., and X.W.D. carried
538 out the wet experiments. Y.-X.H., S.Y.G., and Y.X. analyzed the experiments data, and
539 wrote the manuscript.

540 **Acknowledgements:** This work was supported by the National Key R&D Program of
541 China (2021YFC2100500), and the Natural Science Foundation of China (grant
542 number 32370095). Part of the experiments was carried out in the Biological & Medical
543 Engineering Core Facilities of the Beijing Institute of Technology. We would like to
544 thank Jinyuan Sun for insightful discussions.

545 **Competing interests:** The authors declare no competing interests.

546 **References:**

547 1. Wang, H.H., Isaacs, F.J., Carr, P.A., Sun, Z.Z., Xu, G., Forest, C.R. and Church,

548 G.M. (2009) Programming cells by multiplex genome engineering and
549 accelerated evolution. *Nature*, **460**, 894-898.

550 2. Keasling, J.D. (2010) Manufacturing molecules through metabolic engineering.
551 *Science*, **330**, 1355-1358.

552 3. Xu, P., Li, L., Zhang, F., Stephanopoulos, G. and Koffas, M. (2014) Improving
553 fatty acids production by engineering dynamic pathway regulation and
554 metabolic control. *Proc Natl Acad Sci U S A*, **111**, 11299-11304.

555 4. Xu, X., Li, X., Liu, Y., Zhu, Y., Li, J., Du, G., Chen, J., Ledesma-Amaro, R. and
556 Liu, L. (2020) Pyruvate-responsive genetic circuits for dynamic control of
557 central metabolism. *Nat Chem Biol*, **16**, 1261-1268.

558 5. Cases, I. and de Lorenzo, V. (2005) Promoters in the environment:
559 transcriptional regulation in its natural context. *Nat Rev Microbiol*, **3**, 105-118.

560 6. Jones, J.A., Toparlak Ö, D. and Koffas, M.A. (2015) Metabolic pathway
561 balancing and its role in the production of biofuels and chemicals. *Curr Opin*
562 *Biotechnol*, **33**, 52-59.

563 7. Carr, P.A. and Church, G.M. (2009) Genome engineering. *Nature*
564 *Biotechnology*, **27**, 1151-1162.

565 8. Johns, N.I., Gomes, A.L.C., Yim, S.S., Yang, A., Blazejewski, T., Smillie, C.S.,
566 Smith, M.B., Alm, E.J., Kosuri, S. and Wang, H.H. (2018) Metagenomic mining
567 of regulatory elements enables programmable species-selective gene expression.
568 *Nat Methods*, **15**, 323-329.

569 9. Kang, M.K., Lee, J., Um, Y., Lee, T.S., Bott, M., Park, S.J. and Woo, H.M. (2014)
570 Synthetic biology platform of CoryneBrick vectors for gene expression in
571 Corynebacterium glutamicum and its application to xylose utilization. *Appl*
572 *Microbiol Biotechnol*, **98**, 5991-6002.

573 10. Markley, A.L., Begemann, M.B., Clarke, R.E., Gordon, G.C. and Pfleger, B.F.
574 (2015) Synthetic biology toolbox for controlling gene expression in the
575 cyanobacterium Synechococcus sp. strain PCC 7002. *ACS Synth Biol*, **4**, 595-

576 603.

577 11. Elmore, J.R., Furches, A., Wolff, G.N., Gorday, K. and Guss, A.M. (2017)
578 Development of a high efficiency integration system and promoter library for
579 rapid modification of Pseudomonas putida KT2440. *Metab Eng Commun*, **5**, 1-
580 8.

581 12. He, S., Zhang, Z. and Lu, W. (2023) Natural promoters and promoter
582 engineering strategies for metabolic regulation in Saccharomyces cerevisiae. *J*
583 *Ind Microbiol Biotechnol*, **50**.

584 13. Cazier, A.P. and Blazeck, J. (2021) Advances in promoter engineering: Novel
585 applications and predefined transcriptional control. *Biotechnol J*, **16**, e2100239.

586 14. Alper, H., Fischer, C., Nevoigt, E. and Stephanopoulos, G. (2005) Tuning
587 genetic control through promoter engineering. *Proc Natl Acad Sci U S A*, **102**,
588 12678-12683.

589 15. Hartner, F.S., Ruth, C., Langenegger, D., Johnson, S.N., Hyka, P., Lin-
590 Cereghino, G.P., Lin-Cereghino, J., Kovar, K., Cregg, J.M. and Glieder, A.
591 (2008) Promoter library designed for fine-tuned gene expression in Pichia
592 pastoris. *Nucleic Acids Res*, **36**, e76.

593 16. Redden, H. and Alper, H.S. (2015) The development and characterization of
594 synthetic minimal yeast promoters. *Nat Commun*, **6**, 7810.

595 17. Jensen, P.R. and Hammer, K. (1998) The sequence of spacers between the
596 consensus sequences modulates the strength of prokaryotic promoters. *Appl*
597 *Environ Microbiol*, **64**, 82-87.

598 18. Guiziou, S., Sauveplane, V., Chang, H.J., Clerté, C., Declerck, N., Jules, M. and
599 Bonnet, J. (2016) A part toolbox to tune genetic expression in Bacillus subtilis.
600 *Nucleic Acids Res*, **44**, 7495-7508.

601 19. Kotopka, B.J. and Smolke, C.D. (2020) Model-driven generation of artificial
602 yeast promoters. *Nat Commun*, **11**, 2113.

603 20. Zrimec, J., Fu, X., Muhammad, A.S., Skrekas, C., Jauniskis, V., Speicher, N.K.,

Börlin, C.S., Verendel, V., Chehreghani, M.H., Dubhashi, D. *et al.* (2022) Controlling gene expression with deep generative design of regulatory DNA. *Nat Commun*, **13**, 5099.

21. Wang, Y., Wang, H., Wei, L., Li, S., Liu, L. and Wang, X. (2020) Synthetic promoter design in Escherichia coli based on a deep generative network. *Nucleic Acids Res*, **48**, 6403-6412.

22. Zhang, P., Wang, H., Xu, H., Wei, L., Liu, L., Hu, Z. and Wang, X. (2023) Deep flanking sequence engineering for efficient promoter design using DeepSEED. *Nat Commun*, **14**, 6309.

23. Seo, E., Choi, Y.N., Shin, Y.R., Kim, D. and Lee, J.W. (2023) Design of synthetic promoters for cyanobacteria with generative deep-learning model. *Nucleic Acids Res*, **51**, 7071-7082.

24. Radford, A., Narasimhan, K., Salimans, T. and Sutskever, I. (2018) Improving language understanding by generative pre-training.

25. Radford, A., Wu, J., Child, R., Luan, D., Amodei, D. and Sutskever, I. (2019) Language models are unsupervised multitask learners. *OpenAI blog*, **1**, 9.

26. Brown, T., Mann, B., Ryder, N., Subbiah, M., Kaplan, J.D., Dhariwal, P., Neelakantan, A., Shyam, P., Sastry, G. and Askell, A. (2020) Language models are few-shot learners. *Advances in neural information processing systems*, **33**, 1877-1901.

27. Dalla-Torre, H., Gonzalez, L., Revilla, J.M., Carranza, N.L., Grzywaczewski, A.H., Oteri, F., Dallago, C., Trop, E., Sirelkhatim, H., Richard, G. *et al.* (2023) The Nucleotide Transformer: Building and Evaluating Robust Foundation Models for Human Genomics. *bioRxiv*, 2023.2001.2011.523679.

28. Ji, Y., Zhou, Z., Liu, H. and Davuluri, R.V. (2021) DNABERT: pre-trained Bidirectional Encoder Representations from Transformers model for DNA-language in genome. *Bioinformatics*, **37**, 2112-2120.

29. Fishman, V., Kuratov, Y., Petrov, M., Shmelev, A., Shepelin, D., Chekanov, N.,

632 Kardymon, O. and Burtsev, M. (2023) GENA-LM: A Family of Open-Source
633 Foundational Models for Long DNA Sequences. *bioRxiv*,
634 2023.2006.2012.544594.

635 30. Devlin, J., Chang, M.-W., Lee, K. and Toutanova, K. (2018) Bert: Pre-training
636 of deep bidirectional transformers for language understanding. *arXiv preprint*
637 *arXiv:1810.04805*.

638 31. Khakzad, H., Igashov, I., Schneuing, A., Goverde, C., Bronstein, M. and Correia,
639 B. (2023) A new age in protein design empowered by deep learning. *Cell*
640 *Systems*, **14**, 925-939.

641 32. Min, B., Ross, H., Sulem, E., Veyseh, A.P.B., Nguyen, T.H., Sainz, O., Agirre,
642 E., Heintz, I. and Roth, D. (2023) Recent Advances in Natural Language
643 Processing via Large Pre-trained Language Models: A Survey. *ACM Comput.*
644 *Surv.*, **56**, Article 30.

645 33. Bostrom, K. and Durrett, G. (2020) Byte pair encoding is suboptimal for
646 language model pretraining. *arXiv preprint arXiv:2004.03720*.

647 34. Sanabria, M., Hirsch, J. and Poetsch, A.R. (2023) Distinguishing word identity
648 and sequence context in DNA language models. *bioRxiv*, 2023.2007.
649 2011.548593.

650 35. Su, W., Liu, M.-L., Yang, Y.-H., Wang, J.-S., Li, S.-H., Lv, H., Dao, F.-Y., Yang,
651 H. and Lin, H. (2021) PPD: a manually curated database for experimentally
652 verified prokaryotic promoters. *Journal of Molecular Biology*, **433**, 166860.

653 36. Li, B., Gou, Y., Liu, J.Z., Zhu, H., Zhou, J.T. and Peng, X. (2020) Zero-shot
654 image dehazing. *IEEE Transactions on Image Processing*, **29**, 8457-8466.

655 37. Hanley, J.A. and McNeil, B.J. (1982) The meaning and use of the area under a
656 receiver operating characteristic (ROC) curve. *Radiology*, **143**, 29-36.

657 38. Ko, Y.-S., Kim, J.W., Lee, J.A., Han, T., Kim, G.B., Park, J.E. and Lee, S.Y.
658 (2020) Tools and strategies of systems metabolic engineering for the
659 development of microbial cell factories for chemical production. *Chemical*

*Society Reviews*, **49**, 4615-4636.

39. de Almeida, B.P., Reiter, F., Pagani, M. and Stark, A. (2022) DeepSTARR predicts enhancer activity from DNA sequence and enables the de novo design of synthetic enhancers. *Nature Genetics*, **54**, 613-624.

40. Wang, Z., Liu, Z., Zhang, W., Li, Y., Feng, Y., Lv, S., Diao, H., Luo, Z., Yan, P., He, M. *et al.* (2023) De novo design and optimization of aptamers with AptaDiff. *bioRxiv*, 2023.2011.2025.568693.

41. Ding, N., Zhang, G., Zhang, L., Shen, Z., Yin, L., Zhou, S. and Deng, Y. (2023) Engineering an AI-based forward-reverse platform for the design of cross-ribosome binding sites of a transcription factor biosensor. *Computational and Structural Biotechnology Journal*, **21**, 2929-2939.

42. Kingma, D.P. and Ba, J. (2014) Adam: A method for stochastic optimization. *arXiv preprint arXiv:1412.6980*.

43. Schneider, A., Hommel, G. and Blettner, M. (2010) Linear regression analysis: part 14 of a series on evaluation of scientific publications. *Dtsch Arztebl Int*, **107**, 776-782.

44. Natekin, A. and Knoll, A. (2013) Gradient boosting machines, a tutorial. *Frontiers in neurorobotics*, **7**, 21.

45. Ridgeway, G., Madigan, D. and Richardson, T.S. (1999), *Seventh International Workshop on Artificial Intelligence and Statistics*. PMLR.

46. Breiman, L. (2001) Random forests. *Machine learning*, **45**, 5-32.

47. McDonald, G.C. (2009) Ridge regression. *Wiley Interdisciplinary Reviews: Computational Statistics*, **1**, 93-100.

48. Drucker, H., Burges, C.J., Kaufman, L., Smola, A. and Vapnik, V. (1996) Support vector regression machines. *Advances in neural information processing systems*, **9**.

49. Chen, T. and Guestrin, C. (2016), *Proceedings of the 22nd acm sigkdd*

*international conference on knowledge discovery and data mining*, pp. 785-794.

50. Loh, W.Y. (2011) Classification and regression trees. *Wiley interdisciplinary reviews: data mining and knowledge discovery*, **1**, 14-23.

51. Willmott, C.J. and Matsuura, K. (2005) Advantages of the mean absolute error (MAE) over the root mean square error (RMSE) in assessing average model performance. *Climate research*, **30**, 79-82.

52. Akoglu, H. (2018) User's guide to correlation coefficients. *Turkish journal of emergency medicine*, **18**, 91-93.

# Figures

## TOC

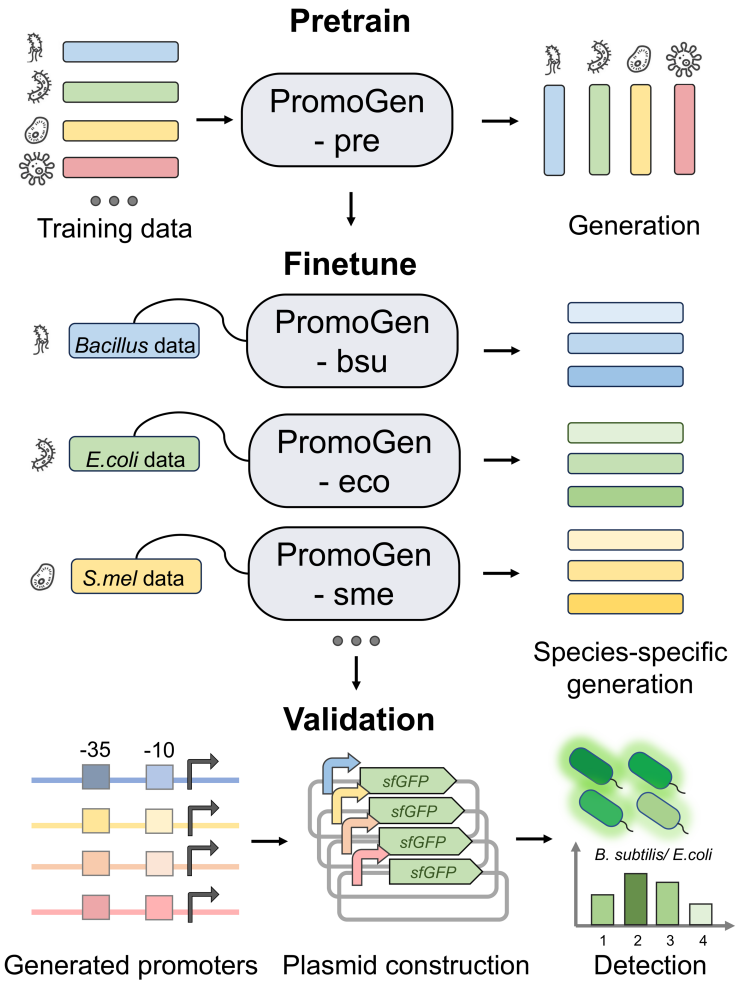
Pretrain
PromoGen - pre
Training data
Generation
Finetune
Bacillus data
PromoGen - bsu
E.coli data
PromoGen - eco
S.mel data
PromoGen - sme
Species-specific generation
Validation
-35
-10
sfGFP
sfGFP
sfGFP
sfGFP
B. subtilis/ E.coli
1
2
3
4
Generated promoters
Plasmid construction
Detection

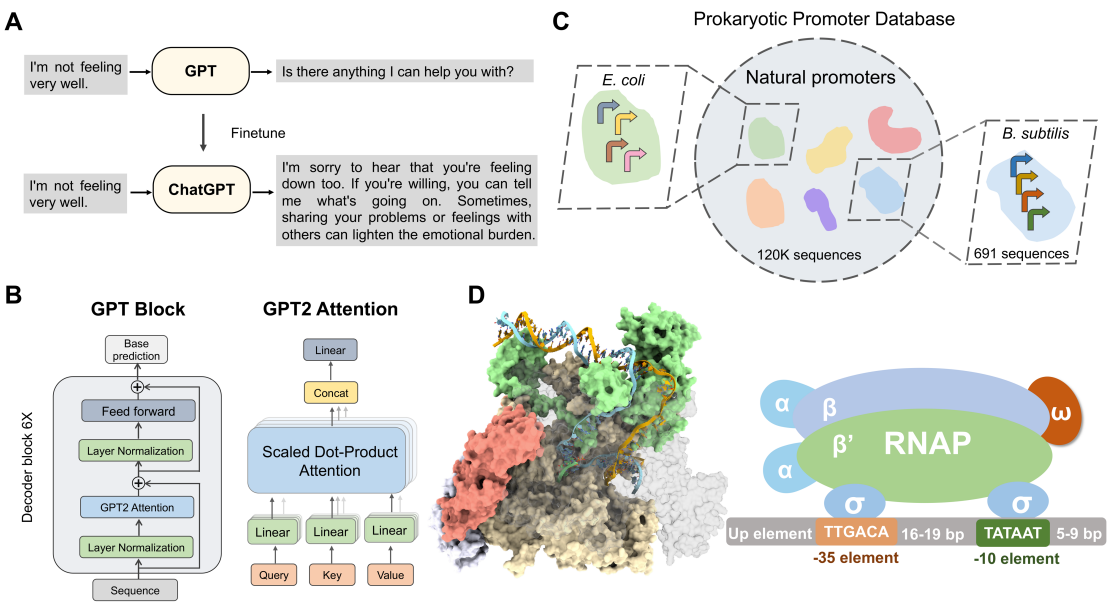


Figure 1. The framework of synthetic promoter design based on nucleotide language model. (A) A pretrained GPT model is capable of generating accurate sentences but may not always align with specific intentions or contexts. By finetuning a pretrained GPT, it can be adapted to not only produce correct sentences but also ensure alignment with the desired intent or context-specific requirements. (B) PromoGen-pre is a 7.4 million parameter neural network based on Transformer architecture, which relies on the self-attention mechanism to capture the distribution of tokens conditioned on context. (C) The PromoGen-pre is trained to generate artificial nucleotide sequence by minimizing the cross-entropy loss on the PPD database. (D) A diagrammatic representation depicts the formation of a transcription initiation complex, comprising promoters and RNA polymerase (RNAP). Promoters are primarily composed of up element, -35 element, flanking sequences, and -10 element. During the assembly of the transcription initiation complex, the α subunit is responsible for anchoring RNAP to the promoter region. The β and β' subunits are involved in recognizing the sigma factor, while the ω subunit assists in the assembly of RNA polymerase.

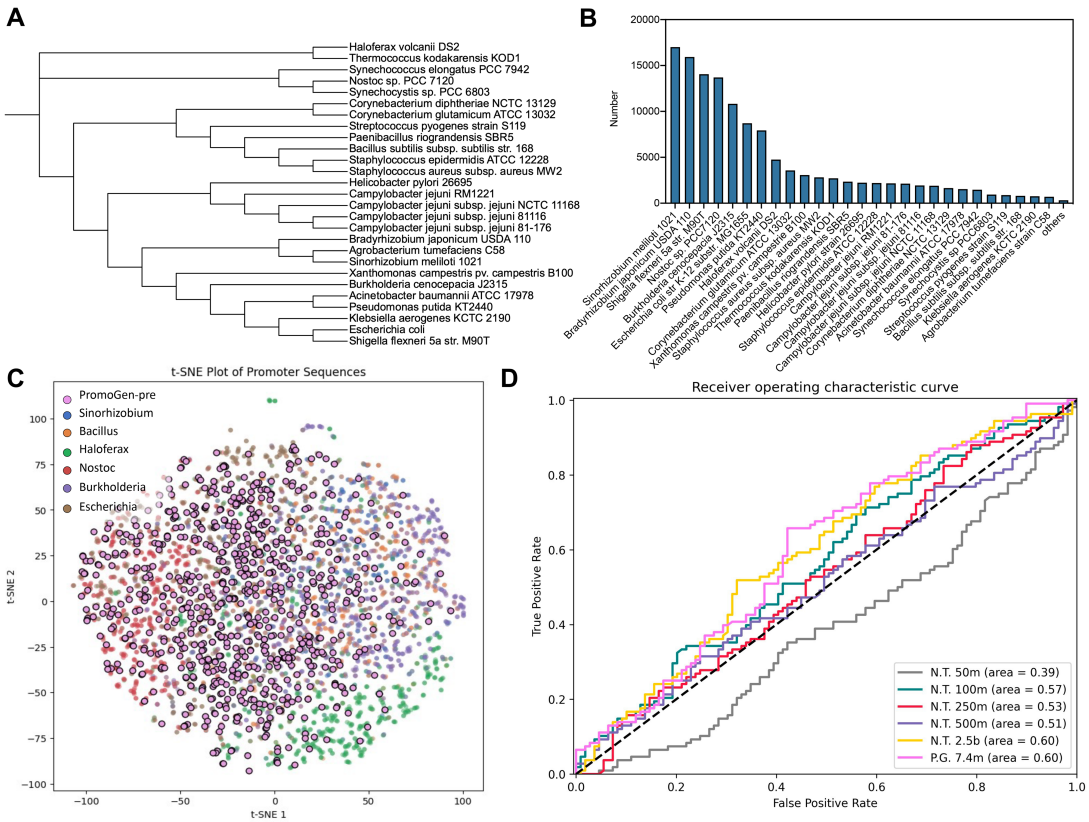


Figure 2. The training of PromoGen-pre. (A) Evolutionary tree of 27 major species included in PPD. (B)The number of promoter sequences contained in each species within PPD. The others indicate the sum of promoters from species except the 27 major ones. (C) The t-SNE, employed as a dimensionality reduction technique, was utilized to illustrate the spatial distribution of both native and generated promoters in a two-dimensional space. The distances between points represent the similarity. Blue, orange, green, red, purple, and grey color points represent the promoter sequences of *Sinorhizobium*, *Bacillus*, *Haloferax*, *Nostoc*, *Burkholderia*, and *Escherichia*, respectively. The pink color points represent the generated sequences of PromoGen. (D) The model likelihoods of PromoGen-pre can accurately predict the activity of generated promoters compared with different parameter sizes of pre-trained nucleotide transformers.

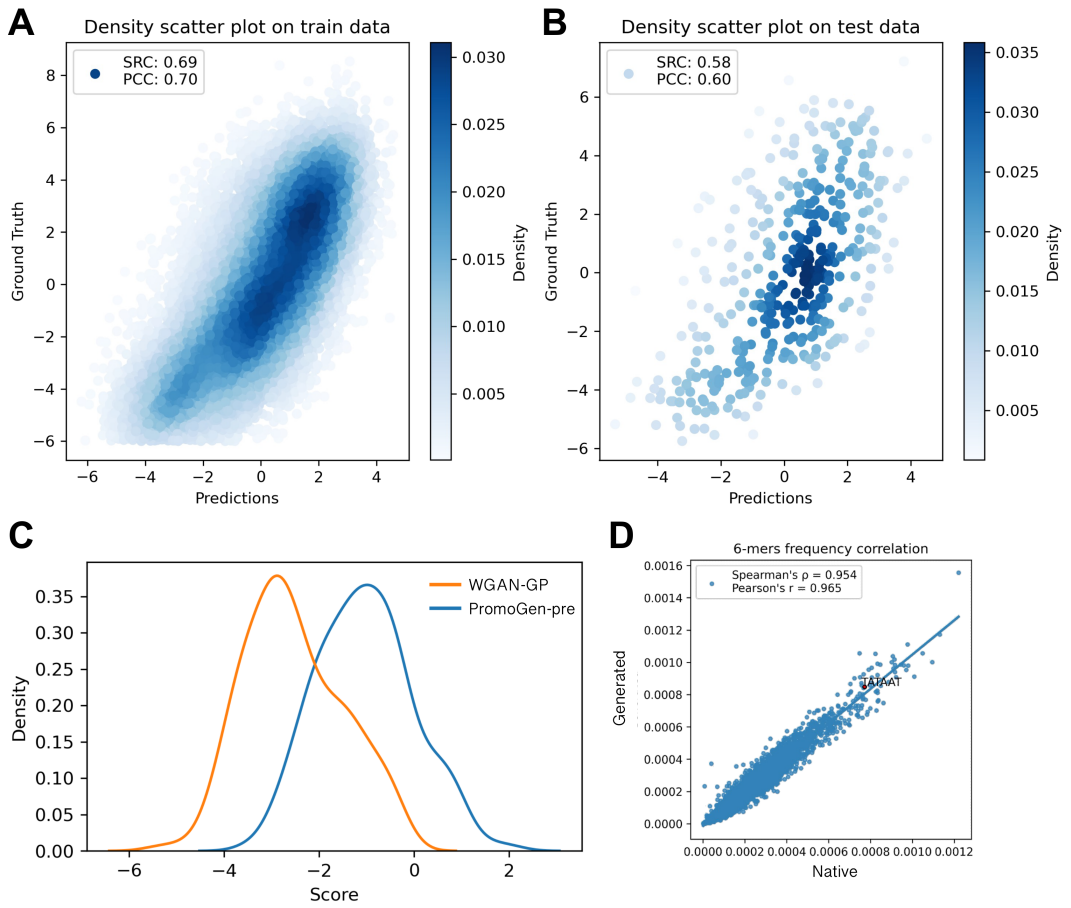


731

732 Figure 3. Comparison of PromoGen-eco with WGAN-GP model. (A) Density scatter
733 plot on train data by Bayesian Bridge prediction model. The depth of color points
734 represents density, with the x-axis and y-axis indicating predicted and actual promoter
735 strengths, respectively. (B) Density scatter plot on test data by Bayesian Bridge
736 prediction model. (C) The distribution of scores in PromoGen-eco and WGAN-GP. The
737 orange and blue color linear represent WGAN-GP and PromoGen-eco, respectively. (D)
738 The 6-mers frequency correlation between native and PromoGen-eco generated
739 promoter sequences. Each data point represents a specific 6-mers, with the x-axis and
740 y-axis indicating the frequency of the 6-mer in native and generated promoters,
741 respectively.

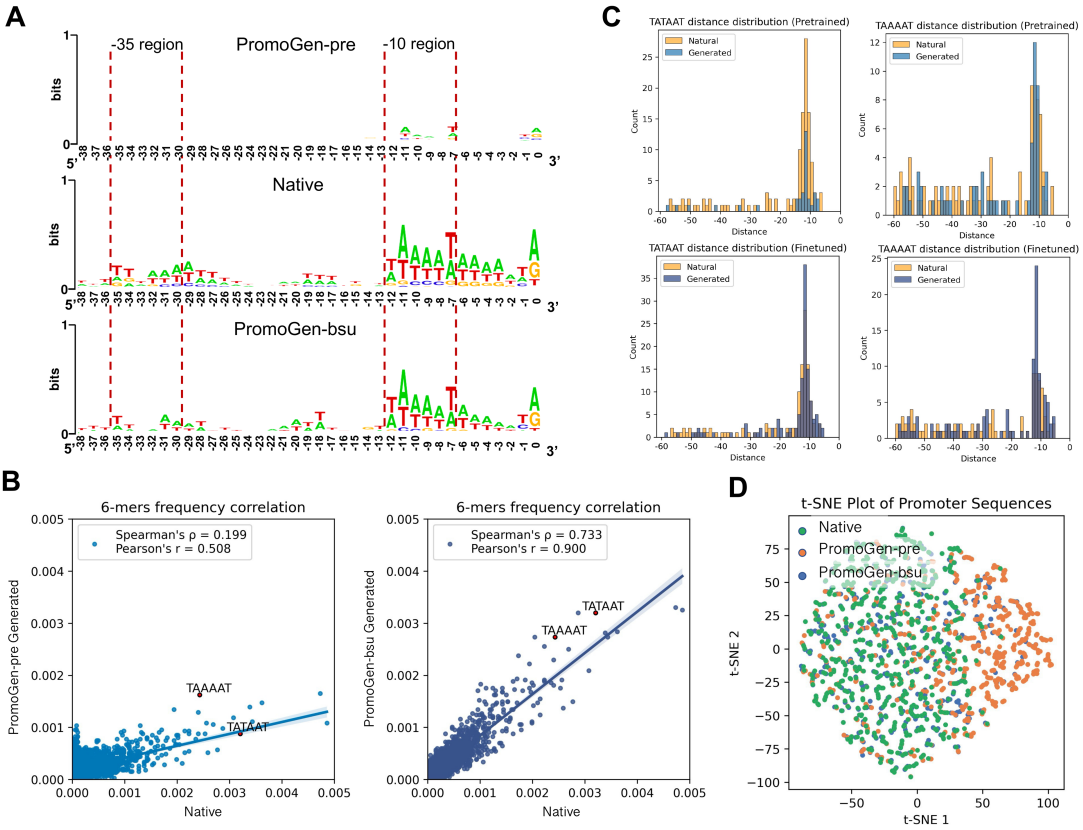


Figure 4. Evaluation of the PromoGen-pre and PromoGen-bsu generated promoters. (A) The sequence logos of the PromoGen-pre-generated, native, and PromoGen-bsu-generated promoters. The 0 represents the transcriptional start site (TSS). The key regions -10 and -35 have been marked by red dotted lines. (B) Spearman and Pearson values were used to assess the frequency of 6-mers between native and generated promoters. Each data point represents a specific 6-mers, with the x-axis and y-axis indicating the frequency of the 6-mer in native and generated promoters, respectively. (C) The distribution patterns of the top two 6-mers in PromoGen-pre and PromoGen-bsu within the -10 regions. The x-axis represents the distance from the TSS, and the y-axis represents the count of the 6-mer at that specific location. (D) The native and generated promoters are visualized in a two-dimensional space, with high-dimensional

data condensed through t-SNE. The distances between points reflect the degree of relevance. Native promoters are depicted as green dots, while PromoGen-pre and PromoGen-bsu generated promoters are represented by orange and blue dots, respectively.

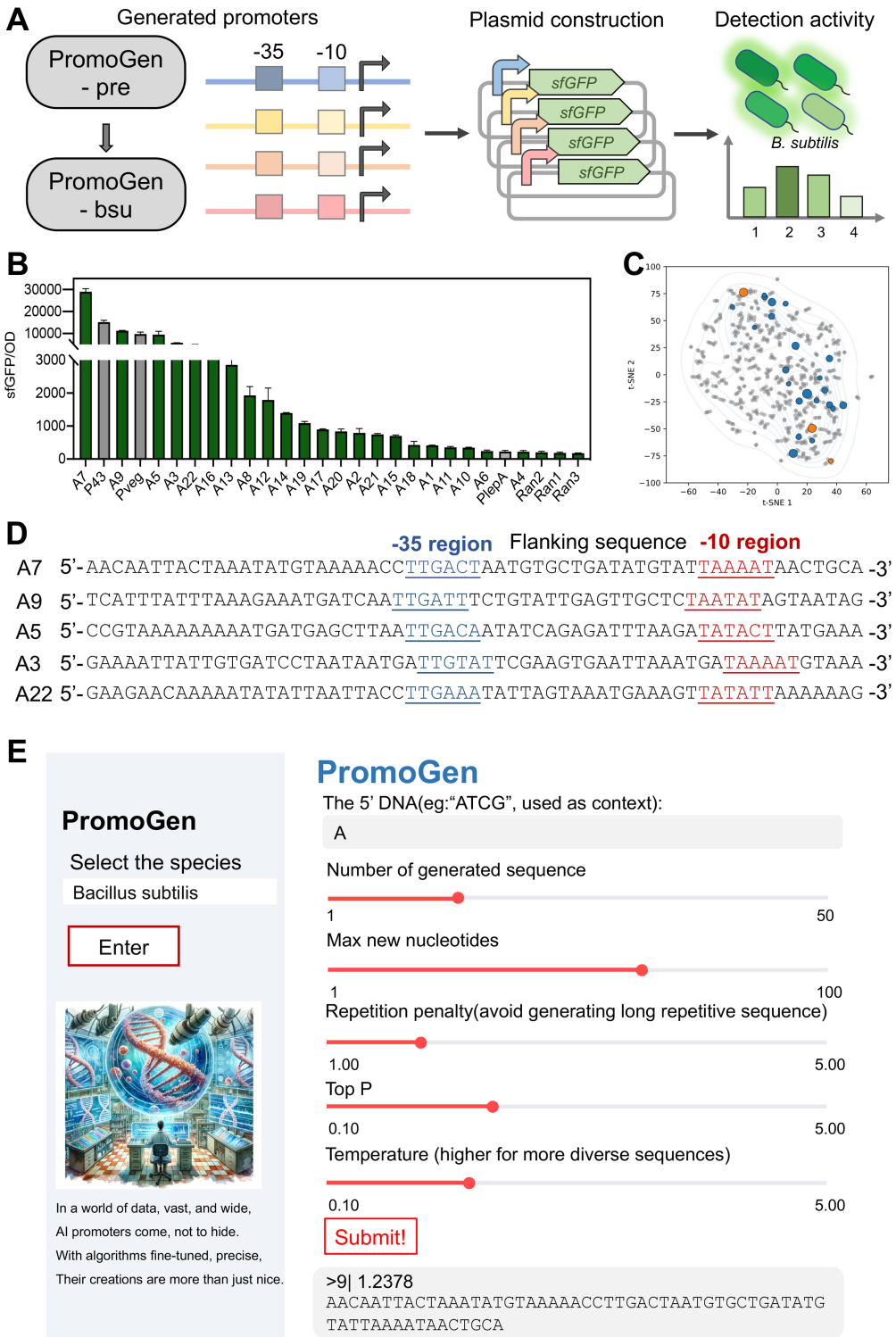


Figure 5. Validation of the generated promoter strength by *sfGFP* expression in *B. subtilis*. (A) Schematic representation of *sfGFP* expression and detection. (B) Strength of promoters were assessed by measuring the fluorescence intensity of *sfGFP* in *B.*

762 *subtilis*. Twenty-two PromoGen-bsu generated promoters were detected, alongside
763 three native promoters ($P_{43}$, $P_{veg}$, $P_{lepA}$) serving as positive controls, and three dummy
764 sequences as negative controls. (C) The native and validation promoters in the
765 embedding spaces. The grey dots represent the 691 native promoters in the dataset. The
766 orange and blue dots represent the native and generated validation promoters. The size
767 of the dots shows the activity of the promoter. (D) The five most active promoters in
768 the experiment were listed. Red and blue characters represent the -10 and -35 regions,
769 respectively. (E) The web server of generate promoter sequences in 27 prokaryotes.
770 When selecting the typical species, certain parameters could be adjusted, including the
771 quantity and length of generated promoter sequences, base repetition penalty, top P and
772 temperature.